Journal of Microbiological Methods 162 (2019) 8–15

Contents lists available at ScienceDirect

Journal of Microbiological Methods

journal homepage: www.elsevier.com/locate/jmicmeth

Customizable 3D printed diffusion chambers for studies of bacterial pathogen phenotypes in complex environments

Lyddia Wilson[a], Kanwal Mohammad Iqbal[d], Terrie Simmons-Ehrhardt[a], Massimo F. Bertino[c], Muhammed Raza Shah[d], Vamsi K. Yadavalli[b], Christopher J. Ehrhardt[a,*]

[a] Department of Forensic Science, Virginia Commonwealth University, Richmond, VA 23284, United States of America
[b] Department of Chemical and Life Science Engineering, Virginia Commonwealth University, Richmond, VA 23284, United States of America
[c] Department of Physics, Virginia Commonwealth University, Richmond, VA 23284, United States of America
[d] H.E.J. Research Institute, University of Karachi, Karachi, Pakistan

ARTICLE INFO

Keywords:
Diffusion chamber
Environmental microbiology
Escherichia coli
Bacillus
Soil microbiology
Atomic force microscopy
FAME profiling

ABSTRACT

Gaps in our understanding of the natural ecology and survival mechanisms of pathogenic bacteria in complex microenvironments such as soil typically occur due to the difficulty in characterizing biochemical profiles and morphological characteristics as they exist in environmental samples. Conversely, accurate simulation of the abiotic and biotic chemistries of soil habitats within the laboratory is often a significant challenge. Herein, we present the fabrication of customizable and precisely engineered 3D printed diffusion chambers that can be used to incubate bacterial cultures directly in soil matrices within a controlled laboratory experiment, and study the dynamics between bacterial cells and soil components. As part of the design process, different types of 3D printing materials were evaluated for ease of sterilization, structural integrity throughout the experiment, as well as cost/ease of production. To demonstrate potential applications for environmental studies, the diffusion chamber was used to incubate cultures of *Bacillus cereus* T-strain and *Escherichia coli* strain O157 directly in soil matrices. We show that the chamber facilitates diffusion of abiotic/biotic components of the soil with target cells without contamination from in situ microbial communities, while allowing for single cell and ensemble level phenotypic analyses of bacteria cultured with and without soil matrices.

1. Introduction

Examining the interactions between microorganisms and environmental matrices in situ continues to be a long standing goal in microbial ecology. For many organisms, propagation using conventional cultivation techniques is difficult, or even impossible in such environmental matrices. Conversely, simulating natural environments in the laboratory for controlled studies is often technically and logistically challenging. One strategy to overcome this is to incubate target organisms within specialized chambers that allow for small non-microbial constituents (i.e. $< 0.2\,\mu m$) to diffuse inside, while preventing the organisms themselves from leaving the chamber. There have been earlier reports using diffusion chambers to study *uncultivable* bacteria in environments ranging from soil (Gavrish et al., 2008; Nichols et al., 2010), to permafrost (Goordial et al., 2017), and seawater (Kaeberlein et al., 2002). Other studies have used diffusion chambers to study microbial survival of microorganisms in similar matrices (McFeters and Stuart, 1972; Vasconcelos and Swartz, 1976). However, in these cases, the specific design and fabrication of the chamber varied with the objectives of the study (i.e., single cell manipulation or aggregate survival), as well as the target environmental matrix.

While most approaches have focused on using diffusion chambers to study typically uncultivable organisms, an unexplored application of diffusion chambers lies in investigating the natural ecology and survival mechanisms of cultivable bacterial pathogens outside of traditional hosts or transmission factors. For instance, for pathogens such as *Bacillus anthracis* (causative agent of anthrax) and *Bacillus cereus* (food poisoning), soil has long been recognized as an important reservoir for spores as well as to facilitate transmission to animal vectors (Turnbull, 2002). Yet, there are potentially complex aspects of the germination/sporulation life cycle that are only recently being investigated (Dey et al., 2012; Schuch and Fischetti, 2009). This is likely owing to the difficulty in accurately simulating abiotic and biotic chemistries of soil habitats within the laboratory (Vilain et al., 2006). Such challenges are amplified if these systems are to be studied in "natural" conditions. For gram-negative pathogens such as *Yersinia pestis*, environmental

* Corresponding author.
E-mail address: cehrhardt@vcu.edu (C.J. Ehrhardt).

https://doi.org/10.1016/j.mimet.2019.05.002
Received 7 March 2019; Received in revised form 3 May 2019; Accepted 3 May 2019
Available online 11 May 2019

matrices such as soil may be an important reservoir contributing to the persistence of natural plague foci and its episodic re-emergence in many parts of the world. Although survival directly in soil has been documented at contaminated field sites as well as in laboratory studies (Eisen et al., 2008; Malek et al., 2017), remarkably little is known about the phenotypic changes that may allow the organisms to survive in such challenging environments. DNA-based surveys have long been used to characterize the abundance and persistence of bacterial pathogens in soil matrices (Campbell et al., 2001; Cheun et al., 2003). However, genetic approaches often provide limited information as to the structural and/or physiological changes that may occur within bacterial pathogens within natural matrices such as soil. As an example, cell size is an important phenotypic characteristic of soil microorganisms that changes in response to limited nutrient availability for endemic soil organisms (Bakken and Olsen, 1987; Portillo et al., 2013). Although bacterial pathogens such as *Y. pestis*, have also been shown to modulate cell size in response to nutrient limited regimes (Pawlowski et al., 2011), this phenotypic transition has not been explicitly investigated for most pathogens within soil matrices. This is due in part, to the sampling requirements for many chemical profiling techniques for bacteria (e.g., proteomics (Nozadze et al., 2015), fatty acid composition (Tan et al., 2010)), coupled with the limited number of techniques for propagating, and then harvesting organisms from environmentally-relevant matrices. The recovery of sufficient numbers of cells (uncontaminated by other bacterial populations) from such environmental studies continues to remain a challenge. The fabrication of new kinds of cell culture chambers that can provide habitats for the controlled exposure of external effectors can be of great importance in such investigations.

In this study we present the design and fabrication of a 3D printed diffusion chamber for studying whole cell phenotypes of bacterial pathogens under complex chemical microenvironments within the laboratory created from incubation in soil matrices. We investigate *Bacillus cereus* T-strain (*Bc*T) and *Escherichia coli* O157:H7 (sub-strain 11,175) as avirulent surrogates for gram positive and gram negative bacterial pathogens, and follow the exposure of soil matrices to such bacteria cultivated within 3D printed growth chambers. We show how the chamber allows for inoculation and harvesting of large numbers of cells for downstream phenotypic analysis. Techniques such as fatty acid profiling (ensemble) and atomic force microscopy (AFM) (single cell) are then used to study the cells obtained from the culture chambers, from a biochemical and morphological perspective. Importantly, the presence of the chamber itself does not affect the cell culture, thereby providing an inbuilt control to study specific external factors. Unlike previously reported devices, we show how 3D printing can be used to custom fabricate these diffusion chambers. This has the potential to offer a durable and low-cost device that can be rapidly and easily manufactured in an 'on demand' fashion. Such 3D printed incubation chambers therefore present a new way to study microbial pathogens for laboratory studies of environmental simulation of in situ processes, and largescale field studies.

2. Methods

2.1. 3D printed incubation chamber

Initially different types of 3D printing materials were investigated: polyamide nylon plastic, stainless steel alloy (60% stainless steel and 40% bronze alloy), polylactic acid, and resin. Chambers with PLA, stainless steel, and nylon plastic materials were printed at Shapeways Inc. (New York, NY). Resin chambers were printed in house using a Form 2 resin printer (Formlabs Inc., Somerville, MA). In the embodiment of the design used in this study, the chamber is fabricated to hold three small agar plugs (40 mm diameter) as the substrate for bacterial inoculation. The agar plugs are held in place by two identical lid pieces with gridded meshes. The 3D model is shown in Fig. 1 and is available as an .stl file for download (https://figshare.com/s/28ac1e46c8ddcf2f7d27).

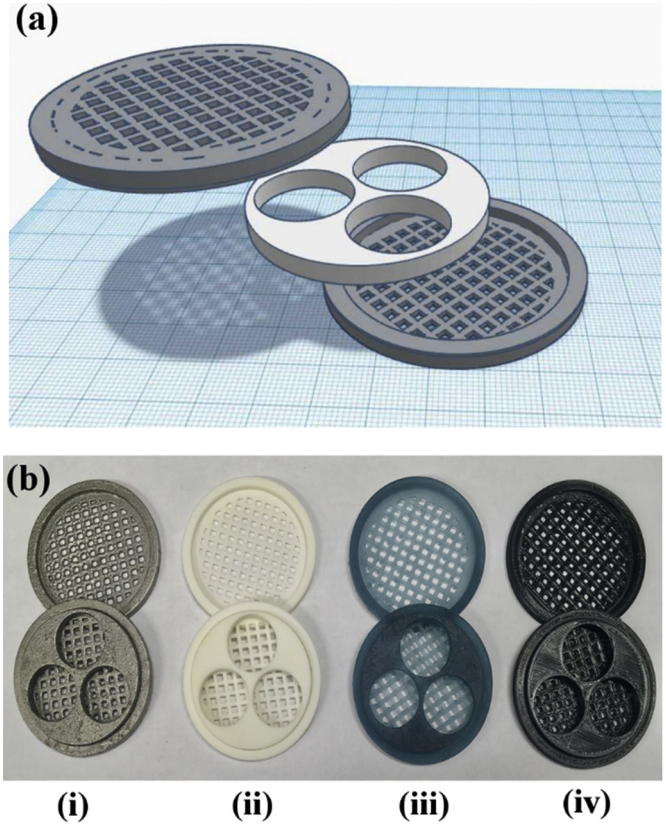

Fig. 1. (a) Diffusion chamber design (b) Diffusion chambers 3D printed in four different materials: (i) stainless steel, (ii) polyamide nylon plastic, (iii) resin, (iv) polylactic acid.

After printing, the three chamber pieces were autoclaved (121 °C, 15 min gravity cycle, jacket pressure 15 psi) and allowed to cool before assembly. Polyethersulfone (PES) membrane filters with 0.03 µm pore size and 60 mm diameter (Sterlitech Corporation, Kent, WA) were fixed to the inside of each lid piece with silicone sealant and allowed to cure for at least four hours. Next, three 40 mm agar plugs were placed inside the inner chamber piece. After inoculating bacteria onto the plugs, the lid pieces were placed above/below the plug assembly. The outer edge was then wrapped in parafilm before incubation within any given matrix (i.e. controlled microenvironment).

As an initial test that the chamber apparatus prevented in situ soil microorganisms from colonizing the agar plugs while still permitting diffusion of chemical components, un-inoculated plugs were sealed inside a series of chambers that were incubated directly in a soil matrix for at least three days. The soil matrix consisted of ~500 g of top soil (upper 5 cm) representing a mixture of organic material and mineral substrates (i.e., O and A soil horizons). This also corresponds with the primary layer(s) of soil with the highest levels of microbial activity and bioturbation and also corresponds to regions where pathogens like *B.anthracis* can persist outside of host. The soil had a deep brown color and a fine sandy loam texture. Quantification of organic matter in soil subsamples was performed using a combustion method (Schumacher, 2002). Results showed organic content ranged between ~5%–10%. After chambers were placed within the soil matrix, deionized water was added to the soil to reach a final water content of 50% within the matrix.

After each incubation period, the plugs were removed from the chamber, and vortexed directly with 5 ml of Tryptic Soy Broth (TSB). The entire broth solution was then plated onto five Tryptic Soy Agar

(TSA) plates (1 ml each) and incubated for 72 h at 30 °C. No colonies were observed on TSA plates. In a subsequent test, uninoculated plugs within a chamber was immersed in a soil matrix and 15 ml of blue-green coloring dye was added to the soil. The chamber with soil was then incubated at 30 °C for 48 h. Following incubation, the agar plugs were removed from the chamber and were observed to be stained with the blue-green dye (Fig. S1; Supplemental Data). Additional experiments to test the permeability of the growth chamber to chemical components of the soil involved adding mammalian blood products to the surrounding soil matrix, and are described below.

2.2. Culturing conditions and viability assays

Testing and development of the chamber was accomplished with two different organisms: *Bacillus cereus* T-strain (*Bc*T) and *Escherichia coli* O157 (sub-strain 11,175). These organisms were chosen due to their structural, genetic, and biochemical similarity to known gram positive and gram negative human pathogens, i.e., *Bacillus anthracis* (Helgason et al., 2000) and *E.coli* O157: H7 (Lim et al., 2010). Because both study organisms are avirulent and classified as Biosafety Level 1, this facilitated easy downstream analyses of single cells using atomic force microscopy (AFM) for this study. *Bc*T and *E.coli* organisms were cultivated independently using separate growth chambers and soil matrices. *E. coli* cultures were initially grown on Tryptic Soy Agar plates (ThermoFisher Scientific, Waltham MA) for 24 h at 37 °C. *B. cereus* were grown on TSA plates for 24 h at 30 °C. For both organisms, one loopful (~10 μl) of each transferred to each agar plug within the growth chamber (Fig. S1). TSA was used as inoculation substrate within the chamber. For *Bc*T chamber culturing experiments, 20 ml of defibrinated sheep's blood (ThermoFisher Scientific, Waltham, MA) was added to the soil matrix to test whether lipid components of the blood could diffuse through the chamber apparatus and associate with the bacterial cultures.

Viability of organisms before and after incubation in the chamber was assessed through plate counts on TSA. Starting cell solutions were created by harvesting one loopful (~10 μl) of bacterial colonies from an overnight TSA culture were resuspended in 5 ml of 1× PBS. Next, 20 μl of this starting cell solution was spread onto each agar plug. After incubation, agar plugs were mixed with 5 ml 1× PBS. Serial dilutions of this cell solution as well as the starter cell solution were then inoculated onto TSA plates (20 μl each). Colonies were counted after incubation for 48 h at 30 °C.

2.3. Fatty acid profiling

Fatty acid profiles for all bacterial samples were generated using the 'Instant FAME' Method following manufacturer's instructions (MIDI Inc. Newark, DE). The protocol utilizes a set of three reagents (part no. 7020; MIDI, Inc., Newark, DE) to extract fatty acids, derivatize to methyl esters, and separate into an organic phase prior to GC analysis. Briefly, ~1 loopful of biomass was added to 250 μl of 'Reagent 1' (KOH-MeOH solution), and vortexed vigorously for five seconds. Next, 125 μl of analytical grade hexane is added followed by another five second vortex. Lastly, 250 μl of 'Reagent 3' (colored aqueous solution) is added to the mixture to enhance the boundary between organic and aqueous phases. Approximately 100 μl of hexane is removed from the top layer and transferred to a new GC vial. Fatty acids were then analyzed with an Agilent 7890A gas chromatograph (GC) using the MIDI Microbial Identification Sherlock software according to the manufacturer's instructions. MIDI calibration standards were used (part no. 1300-C) for identification and quantification of fatty acid peaks.

2.4. Atomic force microscopy

All cells were inactivated using previously reported methanol protocols (Wang et al., 2016). For force spectroscopy, cells were chemically immobilized using APTES and glutaraldehyde on freshly cleaved mica. Briefly, mica slides were incubated in APTES vapor in a vacuum desiccator for 16 h, immersed in 1 ml 2% (*v*/v) glutaraldehyde water solution for 1 h and then rinsed with deionized water. 30 μl of cell suspensions in water (from the chamber cultures) was pipetted out on the modified mica surfaces. Soft gold-coated cantilevers (TR800PB) (spring constant ~0.2 N/m, resonance frequency 40 kHz) and AC 240TS cantilevers (spring constant ~2 N/m, resonance frequency 70 kHz) were used for imaging in air and characterization of the surfaces in non-contact mode. Image analysis was performed using IgorPro and Image J software.

3. Results and discussion

3D printing is rapidly emerging as a valuable tool in scientific investigations. It provides a way to fabricate customizable, on demand devices due to computer aided design, automated, assembly-free fabrication, low cost, and high throughput (Bhattacharjee et al., 2016). However, its use in microbiology and specifically, the fabrication of cell culture devices has not been widely shown. In this study, we demonstrate how a 3D printed diffusion chamber provides an effective device for the culture of cell populations in controlled environments. In addition to the simplicity of creating geometries and controlling the device parameters (e.g. diffusion), it offers the advantage of rapidly moving from design to a finished prototype for use by researchers. The design of the chambers is intended to incubate target organisms, allowing for small non-microbial constituents (i.e. < 0.2 μm) to diffuse inside, while preventing the organisms from leaving the chamber. The number and geometry of the chambers can be easily controlled. Note that the diffusion of the non-microbial constituents can be easily tuned by changing the pore size of the mesh.

3.1. Material selection

Initially, four different printing materials were evaluated for production of the diffusion chamber; polylactic acid (PLA), resin, polyamide nylon plastic, and stainless steel (Fig. 1b). These materials were chosen as common materials that are available to use with a wide range of commercially available 3D printers. The properties of these materials are discussed in Table 1. While all materials were suitable at providing the resolution and moldability to form devices, it is important to test if they can be sterilized for cell culture. As shown earlier using 3D printed thermoplastics, with appropriate handling, these devices are capable of producing sterile components from a non-sterile feedstock (Neches et al., 2016). PLA and resin chambers showed lower heat stability and could not be autoclaved without affecting the physical integrity of

Table 1
Characteristics and properties of 3-D printed materials tested for incubation chamber experiments.

Materials/properties	60% Stainless steel 40%Bronze Alloy	Polyamide	Resin	PLA (Polylactic acid)
Flexibility	None	Moderate	Low	Very Little
Heat tolerance	High ~831 °C	Low /Moderate ~80 °C -160 °C	Low ~100 °C	Low ~110 °C
Cost	Moderate/High	Low	Moderate/High	Low
Sterilization	Moderate	Good	Poor	Poor

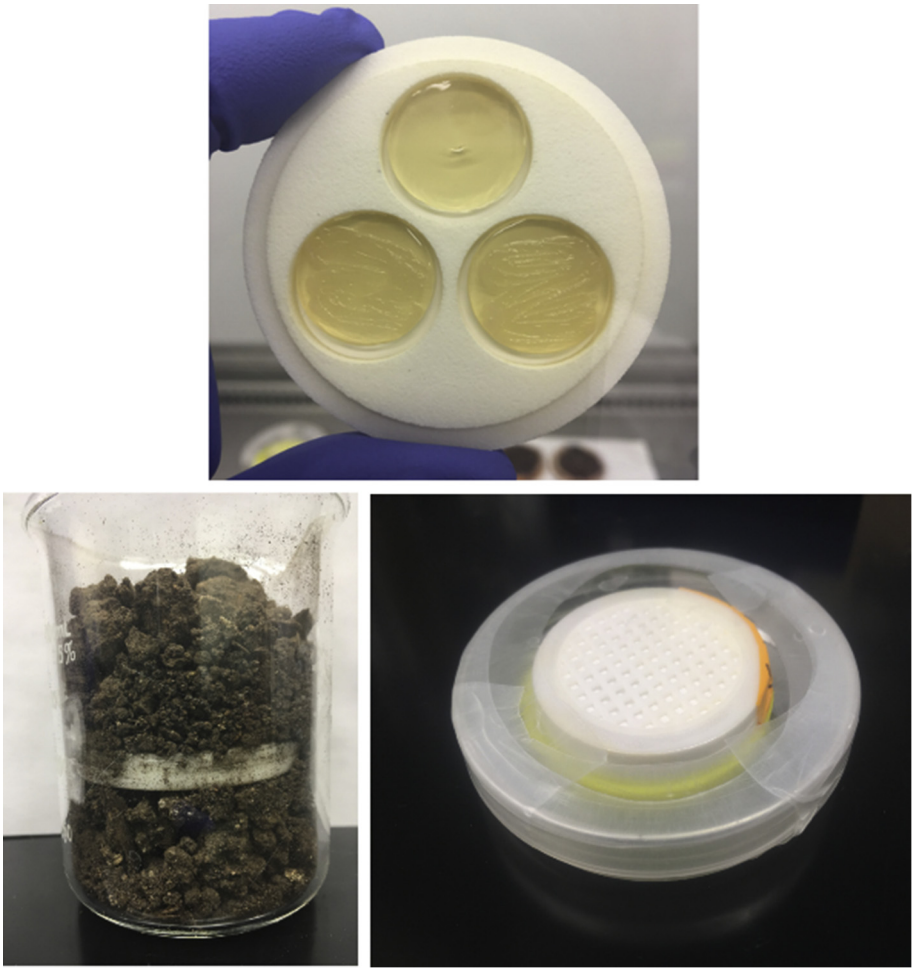

Fig. 2. Inoculation and incubation of diffusion chamber. For these experiments, two of the agar plugs are inoculated with either *B. cereus* or *E. coli* cells. The third plug is not inoculated and serves as a quality control check for microbial contamination from the surrounding matrix (top image). Chamber can be fully immersed within soil matrix (bottom left). For comparison, organisms were also cultivated in the chamber without a surrounding soil matrix (bottom right).

Table 2
Fatty acid composition of *E.coli* O157 grown on TSA within and without diffusion chamber.[a]

	16:1ω7c/ω6c	16:0	17:0 cyclo	18:1 ω7c	18:0	19:0 cyclo ω8c
TSA in chamber (no soil)	5.4 ± 0.6	29.8 ± 6.2	6.4 ± 4.8	29.6 ± 10.6	2.3 ± 1.3	12.7 ± 3.2
TSA in chamber (soil)	7.9 ± 3.0	31.9 ± 1.9	13.2 ± 5.0	33.0 ± 7.0	1.7 ± 0.6	6.9 ± 3.6
TSA plate no chamber	4.0 ± 0.9	28.0 ± 2.4	15.3 ± 0.5	29.9 ± 3.1	1.4 ± 0.2	13.1 ± 3.8

[a] Relative abundance values represent an average of three replicate batch cultures and three GC replicates (n = 9). Standard deviation given for each average value.

individual pieces. In contrast, chambers printed using stainless steel or polyamide nylon were mechanically robust enough to be autoclave sterilized. Immersion in 70% ethanol for 15 min was also tested as a method to sterilize PLA and resin chambers following previous reports (Smith et al., 2011). It was found that microbes could still be recovered from both chamber surfaces after immersion in ethanol for up to 30 min. Although additional sterilization procedures were not examined for PLA and resin, other approaches such as ethylene oxide gas or gamma radiation may prove more effective for these printing materials. For stainless steel chambers, corrosion pits were observed across each chamber component after multiple uses and autoclave sterilization cycles, precluding its use. Therefore, nylon filament was used as the material of choice for all growth chambers in this study. Initial testing using chambers with sterile agar plugs incubated directly in environmental soil matrix showed no evidence of contamination from in situ microbial communities within the chamber. Additionally, colored dyes added to the soil matrix during incubation indicated diffusion of chemical components through the chamber and to the agar plugs (Fig. S1; Supplemental Data).

To investigate the utility of the diffusion chamber for studying the phenotypic transitions of bacterial pathogens in the presence of soil matrix, two different organisms were inoculated in the chamber in separate experiments- *E.coli* O157 and *B.cereus* T-strain (*Bc*T). The chamber was then completely immersed within a soil matrix (Fig. 2). After 48 h, organisms were recovered from the chamber and subjected to fatty acid profiling using GC and morphological analysis using AFM. The effect that the incubation chamber had on organism viability was investigated through enumeration of colony forming units before and after incubation. Results for three experimental replicates of *E.coli* and *B. cereus* showed no systematic change between the starting number of viable organisms added to each agar plug and the number of organisms recovered from each chamber setup, with at least 10^5 organisms

Table 3
Fatty acid composition of *Bacillus cereus* T-strain grown on TSA within and without diffusion chamber.[a]

	13:0 iso	13:0 ante	14:0 iso	15:0 iso	15:0 ante	16:1ω7c	16:0iso	Sm[b]	16:0	17:1 iso ω10c	17:1 iso ω5c	17:0 iso	17:0 ante	18:1ω9c
TSA in chamber (no soil)	9.0 ± 0.8	1.1 ± 0.6	4.1 ± 0.4	32.0 ± 4.7	4.1 ± 1.2	8.5 ± 0.1	5.6 ± 0.1	2.0 ± 0.2	7.3 ± 2.8	4.8 ± 0.7	4.1 ± 0.9	9.2 ± 0.6	1.0 ± 0.2	0.3 ± 0.5
TSA in chamber (Soil with blood)	7.7 ± 0.3	0.6 ± 0.9	4.4 ± 0.5	23.9 ± 6.1	4.7 ± 0.4	7.1 ± 1.0	5.3 ± 0.0	1.8 ± 0.1	11.0 ± 3.6	4.6 ± 1.2	3.4 ± 0.9	7.9 ± 2.8	1.2 ± 0.1	6.9 ± 2.4
TSA Plate no chamber	11.2 ± 1.8	1.9 ± 0.1	4.5 ± 0.4	21.9 ± 4.6	5.7 ± 0.5	6.9 ± 2.8	5.8 ± 1.0	0.7 ± 0.5	16.8 ± 8.5	3.2 ± 2.2	1.3 ± 0.8	8.7 ± 1.6	1.5 ± 0.01	0.3 ± 0.1

[a] Relative abundance values represent an average of three replicate batch cultures and three GC replicates (n = 9). Standard deviation given for each average value.
[b] Represents two fatty acid structures with same retention time using this method: 14:0 3OH, 16:1 iso I.

recovered following incubation (Table S1; Supplemental Data). For each organism, only one replicate trial showed lower numbers of viable cells after chamber incubation compared to the starting cell solution. Further, no clear differences were observed between the number of organisms recovered from chambers immersed in the soil matrix from either chambers incubated without soil, or from agar plugs incubated without the chamber. Differences across culturing replicates may be due in part to heterogeneity among agar plugs and the difficulty spreading cell solutions evenly over a limited area of agar. This could be an important factor when executing viability/CFU assays using this apparatus, particularly for experiments investigating the stability of target organisms over longer periods of time.

3.2. Fatty acid profiling

Fatty acid profiles of *E.coli* cultured on TSA within the diffusion chamber without a surrounding soil matrix were similar to *E.coli* harvested from a standard TSA plate (Table 2) across several of the most abundant FAME biomarkers including 16:1 ω7c, 16:0, 18:1 ω7c, 18:0, and 19:0 cyclo ω8c (Table 2). The only marked difference observed was in the abundance of 17:0 cyclo (6.4 ± 4.8 for chamber and 15.3 ± 0.5 for TSA). Additionally, certain fatty acids showed more variability between culture replicates in TSA growth chamber samples compared to TSA plates (e.g., 16:0, 17:0 cyclo; 18:1 ω7c). These differences between growth on TSA with and without the chamber may be largely a function of the available surface area of the agar in each culture; 40 mm diameter agar plug within the chamber and 100 mm diameter agar in a standard media plate. Since less biomass is harvested from agar plugs within the chamber, these samples may exhibit more phenotypic heterogeneity compared to standard TSA plates, where phenotypic differences are likely to be mitigated by harvesting biomass across a larger area prior to fatty acid extraction and profiling (Jeanson et al., 2015).

Comparison of fatty acid profiles between cultures grown in the diffusion chamber with and without surrounding soil matrix showed similar abundance of 16:0, 18:1 ω7c, and 18:0 biomarkers (Table 2). Cultures grown with soil matrix were slightly enriched in 17:0 cyclo and depleted in 19:0 cyclo ω7c, in comparison to cultures grown without soil. However, due to the overlapping range of values and generally higher variation in the abundance of these biomarkers and their biosynthetic precursors (e.g., 16:0), it is unclear whether these difference are due to incubation in soil, or due to heterogeneity among replicates.

For *B.cereus* cultures, the relative abundance of many fatty acid biomarkers were largely consistent across chamber cultures (with and without soil) as well as cultures taken from a conventional TSA plate (e.g., 13:0 anteiso, 14:0 iso; 15:0 anteiso, 16:0 iso; Table 2). Certain fatty acids show differences between chamber cultures without soil and TSA plates, including 15:0 iso, 16:0, and 17:1 iso ω5c. The high variance of these biomarkers across replicates may reflect intrinsic heterogeneity in these biomarkers both across cultures and within the same agar sample. One fatty acid, 18:1 ω9c, was only observed in *B.cereus* incubated in soil inoculated with sheep's blood (Table 3). This fatty acid is not a known taxonomic biomarker for the *Bacillus* ACT group and has been observed to occur in *Bc*T profiles only when grown directly on blood-supplemented agar media (Ehrhardt et al., 2010). This combined with the fact that chamber agar plugs incubated with blood supplemented soil were stained visibly red (Fig. S2; Supplemental Data), indicates that components of the soil are able to diffuse through the chamber and interact with cells on the inner agar substrate.

3.3. Morphological imaging using atomic force microscopy (AFM)

Cell size is a key ecological trait of microorganisms that can determine a range of life history attributes, including the efficiency of nutrient acquisition (Bakken and Olsen, 1987). Cells were imaged using atomic force microscopy (AFM) to observe the cell size, morphology,

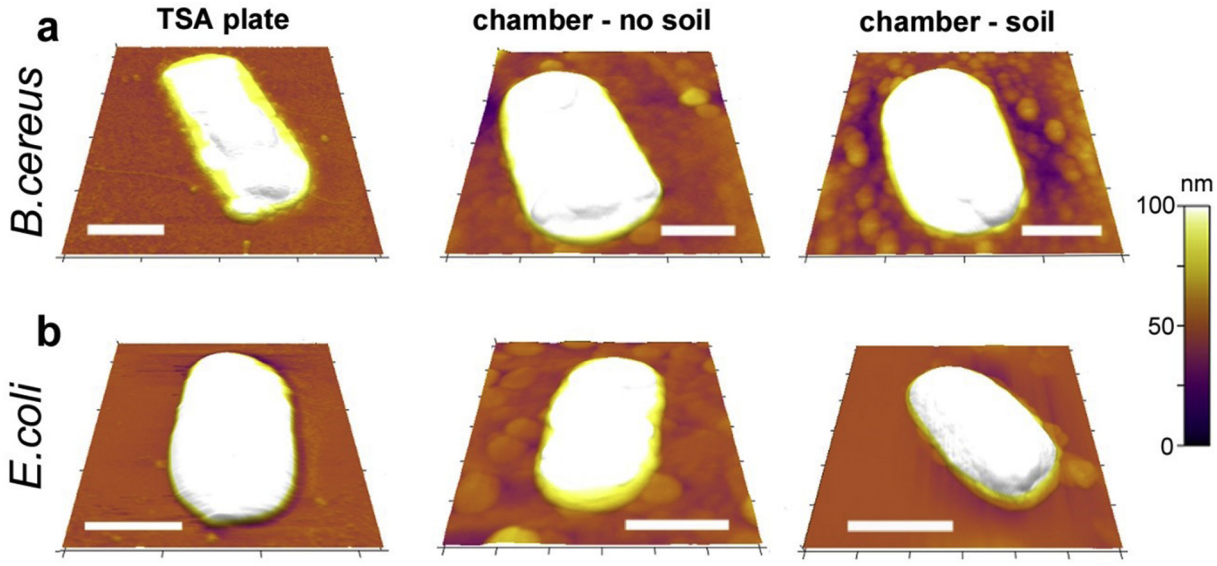

Fig. 3. Representative AFM images showing the (a) *B. cereus* and (b) *E. coli* grown under different conditions. Bacterial cells grown on TSA plate (no soil) can be compared directly with cells grown in the diffusion chamber but in the absence of soil. These two can be compared with the cells cultured in soil in the diffusion chamber. All images have been presented to the same z-scale to facilitate comparison. Scale bar = 1 μm on all panels. Note that the *E. coli* (lower panel) are at 3 μm total scan area for better visibility (larger *B. cereus* are at 4 μm scan area).

Table 4
Morphological analysis of the cells grown in the chamber.

	Length (μm)	Width (μm)	Area (μm^2)
*Bc*T cells without soil	4.0 ± 0.4	1.8 ± 0.2	5.8 ± 1.3
*Bc*T cells in chamber without soil	3.8 ± 0.3	1.8 ± 0.25	5.6 ± 0.9
*Bc*T cells in chamber with soil	3.0 ± 0.45	1.6 ± 0.3	4.1 ± 1.1
E. coli cells without soil	2.7 ± 0.6	1.2 ± 0.05	2.8 ± 0.7
E. coli cells in chamber without soil	2.6 ± 0.3	1.5 ± 0.1	3.0 ± 0.4
E. coli cells in chamber with soil	2.3 ± 0.45	1.4 ± 0.1	2.5 ± 0.9

and surface topography at the single cell level. The AFM is an important and widely used tool in microbiology (Dufrêne, 2008; Dupres et al., 2010; Müller and Dufrêne, 2011). The unique advantage of the AFM is the ability to characterize cellular surfaces with nanoscale resolution and 3D imaging (Plomp et al., 2007). Samples for AFM do not require preparative steps such as dye staining, fluorescence labeling, conductive coating or vacuum, and can be measured under near physiological environments (Fernandes et al., 2009; Gillis et al., 2012). Over the past decade, there have several AFM studies on bacteria including high resolution nanoscale imaging, (Kailas et al., 2011; Plomp et al., 2005) and observing how antibacterial ingredients or harsh conditions affect the morphology and mechanical properties, (Fernandes et al., 2009; Xing et al., 2014). AFM based techniques have been previously applied for specifically imaging and characterizing bacterial processes (Liu and Wang, 2010; Wang et al., 2015a,b).

In these experiments, AFM imaging was conducted to achieve two objectives: a) verify that the diffusion chamber itself did not affect the cell morphology, and b) observe the effect of the soil culture on the bacteria. Since the numbers of cells grown in these chambers is relatively small, analysis is constrained to tools such as the AFM that permit investigations at the single cell level. Initially, cells grown on TSA were compared with cells grown within the diffusion chambers, but in the absence of soil. These samples also served as a control for organisms incubated in the presence of soil matrix. The nanoscale surface morphology of cells under different conditions are shown in Fig. 3 as representative AFM images. Both sets of cells showed characteristic structures as expected (e.g. rod-shaped morphology). A quantitative analysis was performed on several cell samples (typically 3–5 cells were studied for each condition). The following parameters were analyzed: cell length, width and area, to compare the cells. As may be seen from the figure and the quantitative data (Table 4), cells grown with and without the chamber were very similar to each other, showing that the chamber itself did not affect the cells. For instance, the *BcT* cells were 4.0 ± 0.4 μm in length, 1.8 ± 0.2 μm in width and area of 5.8 ± 1.3 μm^2, consistent with previously reported dimensions (Fernandes et al., 2009; Pan et al., 2006). Cells grown in the diffusion chambers, showed a length of 3.8 ± 0.3 μm, width of 1.8 ± 0.25 μm and area of 5.6 ± 0.9 μm^2. A similar trend was observable with the *E. coli* cells (area with and without chamber - 2.8 ± 0.7 μm^2 and 3.0 ± 0.4 μm^2 respectively). Height profiles of cells measured along the "long axis" of cells, showed that the cells in and without the chamber were the same height, whereas cells in soil were slightly more rounded.

The next set of experiments was designed to study the phenotypic changes of the cells after exposure to soil environments. For this, bacteria cultured in the diffusion chambers in the presence of soil were collected for imaging. As seen in Fig. 3 and Table 4, cultivation with surrounding soil matrix results in ~25% smaller cells in the case of *Bc*T - 4.1 ± 1.1 μm^2, vs. ~16% smaller cells in the case of *E. coli* 2.5 ± 0.9 μm^2. This is consistent with several studies which have shown that bacterial cultures in soil tend to be smaller (Bakken and Olsen, 1987; Portillo et al., 2013). This has been attributed to the fact that nutrient deprivation can reduce cell size (Young, 2006). Cell sizes in soil are generally smaller than cell sizes typically measured for the most commonly studied isolates grown under laboratory conditions (Bakken and Olsen, 1987; Portillo et al., 2013). In fact, a majority of soil bacteria themselves (as opposed to the comparison of bacteria grown in soil) are < 0.5 μm in diameter (Bakken and Olsen, 1987). This is an important consideration in the design and selection of appropriate filters for various taxa studied in the 3D printed chambers discussed in this work. The ease of conducting the cell culture in the diffusion chamber, coupled with the facile collection and minimization of contamination from other populations, present distinct advantages of this system. Finally, we note that the pore size of the PES membrane filter could be altered to selectively include/exclude certain soil constituents from the chamber such as bacterial spores, mineral particles, or bacteriophages (< 200 nm). Bacteriophages in particular have been

implicated as mediating phenotypic transitions of *Bacillus* ACT organisms within the soil (Schuch and Fischetti, 2009) and may be a useful area of investigation for in situ studies using this approach.

4. Conclusions

In this report, we have presented a novel 3D printed diffusion chamber for studying the interactions of bacterial cells with complex microenvironments. The chambers can be custom designed and rapidly printed using a variety of materials at low cost. Initial tests with *E.coli* and *B.cereus* show that the chamber permits diffusion of abiotic/biotic soil components to inner agar culture without contamination from in situ organisms. Importantly, biochemical and morphological phenotypes can be successfully analyzed from target cells after incubation in soil matrix. While the goal of this study is to present the design and optimize the chamber for controlled soil incubations using analogs for environmentally-relevant bacterial pathogens, the small size and sterilizable nature of the chamber makes it amenable to similar laboratory-based studies using virulent bacterial pathogens classified at Biosafety Level 2 or Biosafety Level 3. These could therefore provide new tools for investigating the survival and long-term persistence of biothreat agents in soil, the effect that exposure to soil matrices has on specific virulence factors, the overall pathogenicity of the organism, or the role that biofilms may have in the ecology of bacterial pathogens within these environments.

Acknowledgements

This work was supported by Cooperative Biological Engagement Program, grant HDTRA1-16-1-0051.

Competing interests

The authors declare no competing interests.

Author contributions

L.W. performed bacterial culturing and fatty acid profiling. K.M.I conducted AFM analyses. T.S.E. designed the chamber and 3D printed initial prototypes for testing and optimization. M.F·B, M.R.S., V.K.Y., and C.J.E. designed and supervised the project. C.J.E. and V.K.Y. prepared the manuscript.

Data availability

All primary data for this study is available at: http://10.6084/m9.figshare.704041

Appendix A. Supplementary data

Supplementary data to this article can be found online at https://doi.org/10.1016/j.mimet.2019.05.002.

References

Bakken, L.R., Olsen, R.A., 1987. The relationship between cell size and viability of soil bacteria. Microb. Ecol. 13, 103–114. https://doi.org/10.1007/BF02011247.

Bhattacharjee, N., Urrios, A., Kang, S., Folch, A., 2016. The upcoming 3D-printing revolution in microfluidics. Lab Chip 16, 1720–1742. https://doi.org/10.1039/c6lc00163g.

Campbell, G.R., Prosser, J., Glover, A., Killham, K., 2001. Detection of Escherichia coli O157:H7 in soil and water using multiplex PCR. J. Appl. Microbiol. 91, 1004–1010. https://doi.org/10.1046/j.1365-2672.2001.01465.x.

Cheun, H.I., Makino, S.I., Watarai, M., Erdenebaatar, J., Kawamoto, K., Uchida, I., 2003. Rapid and effective detection of anthrax spores in soil by PCR. J. Appl. Microbiol. 95, 728–733. https://doi.org/10.1046/j.1365-2672.2003.02038.x.

Dey, R., Hoffman, P.S., Glomski, I.J., 2012. Germination and amplification of anthrax spores by soil-dwelling amoebas. Appl. Environ. Microbiol. 78, 8075–8081. https://doi.org/10.1128/AEM.02034-12.

Dufrêne, Y.F., 2008. Towards nanomicrobiology using atomic force microscopy. Nat Rev Microbiol 6, 674–680. https://doi.org/10.1038/nrmicro1948.

Dupres, V., Alsteens, D., Andre, G., Dufrêne, Y.F., 2010. Microbial nanoscopy: a closer look at microbial cell surfaces. Trends Microbiol. 18, 397–405. https://doi.org/10.1016/j.tim.2010.06.004.

Ehrhardt, C.J., Chu, V., Brown, T., Simmons, T.L., Swan, B.K., Bannan, J., Robertson, J.M., 2010. Use of fatty acid methyl ester profiles for discrimination of Bacillus cereus T-strain spores grown on different media. Appl. Environ. Microbiol. 76, 1902–1912. https://doi.org/10.1128/AEM.02443-09.

Eisen, R.J., Petersen, J.M., Higgins, C.L., Wong, D., Levy, C.E., Mead, P.S., Schriefer, M.E., Griffith, K.S., Gage, K.L., Beard, C.B., 2008. Persistence of Yersinia pestis in soil under natural conditions. Emerging Infect Dis 14, 941–943. https://doi.org/10.3201/eid1406.080029.

Fernandes, J.C., Eaton, P., Gomes, A.M., Pintado, M.E., Xavier Malcata, F., 2009. Study of the antibacterial effects of chitosans on Bacillus cereus (and its spores) by atomic force microscopy imaging and nanoindentation. Ultramicroscopy 109, 854–860. https://doi.org/10.1016/j.ultramic.2009.03.015.

Gavrish, E., Bollmann, A., Epstein, S., Lewis, K., 2008. A trap for in situ cultivation of filamentous actinobacteria. J. Microbiol. Methods 72, 257–262. https://doi.org/10.1016/j.mimet.2007.12.009.

Gillis, A., Dupres, V., Delestrait, G., Mahillon, J., Dufrêne, Y.F., 2012. Nanoscale imaging of Bacillus thuringiensis flagella using atomic force microscopy. Nanoscale 4, 1585–1591. https://doi.org/10.1039/c1nr11161b.

Goordial, J., Altshuler, I., Hindson, K., Chan-Yam, K., Marcolefas, E., Whyte, L.G., 2017. In situ field sequencing and life detection in remote (79°26'N) canadian high arctic permafrost ice wedge microbial communities. Front. Microbiol. 8, 2594. https://doi.org/10.3389/fmicb.2017.02594.

Helgason, E., Okstad, O.A., Caugant, D.A., Johansen, H.A., Fouet, A., Mock, M., Hegna, I., Kolstø, A.B., 2000. Bacillus anthracis, Bacillus cereus, and Bacillus thuringiensis–one species on the basis of genetic evidence. Appl. Environ. Microbiol. 66, 2627–2630.

Jeanson, S., Floury, J., Gagnaire, V., Lortal, S., Thierry, A., 2015. Bacterial colonies in solid media and foods: a review on their growth and interactions with the micro-environment. Front. Microbiol. 6, 1284. https://doi.org/10.3389/fmicb.2015.01284.

Kaeberlein, T., Lewis, K., Epstein, S.S., 2002. Isolating "uncultivable" microorganisms in pure culture in a simulated natural environment. Science 296, 1127–1129. https://doi.org/10.1126/science.1070633.

Kailas, L., Terry, C., Abbott, N., Taylor, R., Mullin, N., Tzokov, S.B., Todd, S.J., Wallace, B.A., Hobbs, J.K., Moir, A., Bullough, P.A., 2011. Surface architecture of endospores of the Bacillus cereus/anthracis/thuringiensis family at the subnanometer scale. Proc. Natl. Acad. Sci. U. S. A. 108, 16014–16019. https://doi.org/10.1073/pnas.1109419108.

Lim, J.Y., Yoon, J., Hovde, C.J., 2010. A brief overview of Escherichia coli O157:H7 and its plasmid O157. J. Microbiol. Biotechnol. 20, 5–14.

Liu, S., Wang, Y., 2010. Application of AFM in microbiology: a review. Scanning 32, 61–73. https://doi.org/10.1002/sca.20173.

Malek, M.A., Bitam, I., Levasseur, A., Terras, J., Gaudart, J., Azza, S., Flaudrops, C., Robert, C., Raoult, D., Drancourt, M., 2017. Yersinia pestis halotolerance illuminates plague reservoirs. Sci. Rep. 7, 40022. https://doi.org/10.1038/srep40022.

McFeters, G.A., Stuart, D.G., 1972. Survival of coliform bacteria in natural waters: field and laboratory studies with membrane-filter chambers. Appl. Microbiol. 24, 805–811.

Müller, D.J., Dufrêne, Y.F., 2011. Atomic force microscopy: a nanoscopic window on the cell surface. Trends Cell Biol. 21, 461–469. https://doi.org/10.1016/j.tcb.2011.04.008.

Neches, R.Y., Flynn, K.J., Zaman, L., Tung, E., Pudlo, N., 2016. On the intrinsic sterility of 3D printing. PeerJ 4, e2661. https://doi.org/10.7717/peerj.2661.

Nichols, D., Cahoon, N., Trakhtenberg, E.M., Pham, L., Mehta, A., Belanger, A., Kanigan, T., Lewis, K., Epstein, S.S., 2010. Use of ichip for high-throughput in situ cultivation of "uncultivable" microbial species. Appl. Environ. Microbiol. 76, 2445–2450. https://doi.org/10.1128/AEM.01754-09.

Nozadze, M., Zhgenti, E., Meparishvili, M., Tsverava, L., Kiguradze, T., Chanturia, G., Babuadze, G., Kekelidze, M., Bakanidze, L., Shutkova, T., Imnadze, P., Francesconi, S.C., Obiso, R., Solomonia, R., 2015. Comparative proteomic studies of Yersinia pestis strains isolated from natural foci in the republic of Georgia. Front. Public Health 3, 239. https://doi.org/10.3389/fpubh.2015.00239.

Pan, J., Ge, X., Liu, R., Tang, H., 2006. Characteristic features of Bacillus cereus cell surfaces with biosorption of Pb(II) ions by AFM and FT-IR. Colloids Surf B Biointerfaces 52, 89–95. https://doi.org/10.1016/j.colsurfb.2006.05.016.

Pawlowski, D.R., Metzger, D.J., Raslawsky, A., Howlett, A., Siebert, G., Karalus, R.J., Garrett, S., Whitehouse, C.A., 2011. Entry of Yersinia pestis into the viable but nonculturable state in a low-temperature tap water microcosm. PLoS One 6, e17585. https://doi.org/10.1371/journal.pone.0017585.

Plomp, M., Leighton, T.J., Wheeler, K.E., Hill, H.D., Malkin, A.J., 2007. In vitro high-resolution structural dynamics of single germinating bacterial spores. Proc. Natl. Acad. Sci. U. S. A. 104, 9644–9649. https://doi.org/10.1073/pnas.0610626104.

Plomp, M., Leighton, T.J., Wheeler, K.E., Malkin, A.J., 2005. The high-resolution architecture and structural dynamics of Bacillus spores. Biophys. J. 88, 603–608. https://doi.org/10.1529/biophysj.104.049312.

Portillo, M.C., Leff, J.W., Lauber, C.L., Fierer, N., 2013. Cell size distributions of soil bacterial and archaeal taxa. Appl. Environ. Microbiol. 79, 7610–7617. https://doi.org/10.1128/AEM.02710-13.

Schuch, R., Fischetti, V.A., 2009. The secret life of the anthrax agent Bacillus anthracis: bacteriophage-mediated ecological adaptations. PLoS One 4, e6532. https://doi.org/10.1371/journal.pone.0006532.

Schumacher, B.A., 2002. Methods for Determination of Total Organic Carbon (TOC) in Soils and Sediments.

Smith, P.N., Palenik, C.J., Blanchard, S.B., 2011. Microbial contamination and the sterilization/disinfection of surgical guides used in the placement of endosteal implants. Int. J. Oral Maxillofac. Implants 26, 274–281.

Tan, Y., Wu, M., Liu, H., Dong, X., Guo, Z., Song, Z., Li, Y., Cui, Y., Song, Y., Du, Z., Yang, R., 2010. Cellular fatty acids as chemical markers for differentiation of Yersinia pestis and Yersinia pseudotuberculosis. Lett. Appl. Microbiol. 50, 104–111. https://doi.org/10.1111/j.1472-765X.2009.02762.x.

Turnbull, P.C., 2002. Introduction: anthrax history, disease and ecology. Curr. Top. Microbiol. Immunol. 271, 1–19.

Vasconcelos, G.J., Swartz, R.G., 1976. Survival of bacteria in seawater using a diffusion chamber apparatus in situ. Appl. Environ. Microbiol. 31, 913–920.

Vilain, S., Luo, Y., Hildreth, M.B., Brözel, V.S., 2006. Analysis of the life cycle of the soil saprophyte Bacillus cereus in liquid soil extract and in soil. Appl. Environ. Microbiol. 72, 4970–4977. https://doi.org/10.1128/AEM.03076-05.

Wang, C., Ehrhardt, C.J., Yadavalli, V.K., 2015a. Single cell profiling of surface carbohydrates on Bacillus cereus. J. R. Soc. Interface 12. https://doi.org/10.1098/rsif.2014.1109.

Wang, C., Ehrhardt, C.J., Yadavalli, V.K., 2016. Nanoscale imaging and hydrophobicity mapping of the antimicrobial effect of copper on bacterial surfaces. Micron 88, 16–23. https://doi.org/10.1016/j.micron.2016.05.005.

Wang, C., Stanciu, C., Ehrhardt, C.J., Yadavalli, V.K., 2015b. Morphological and mechanical imaging of Bacillus cereus spore formation at the nanoscale. J. Microsc. 258, 49–58. https://doi.org/10.1111/jmi.12214.

Xing, Y., Li, A., Felker, D.L., Burggraf, L.W., 2014. Nanoscale structural and mechanical analysis of Bacillus anthracis spores inactivated with rapid dry heating. Appl. Environ. Microbiol. 80, 1739–1749. https://doi.org/10.1128/AEM.03483-13.

Young, K.D., 2006. The selective value of bacterial shape. Microbiol. Mol. Biol. Rev. 70, 660–703. https://doi.org/10.1128/MMBR.00001-06.